Journal of Catalysis 270 (2010) 249–255

Contents lists available at ScienceDirect

Journal of Catalysis

journal homepage: www.elsevier.com/locate/jcat

Kinetic stability of nitrogen-substituted sites in HY and silicalite from first principles

Vishal Agarwal [a], George W. Huber [a], W. Curtis Conner Jr. [a], Scott M. Auerbach [a,b,*]

[a] Department of Chemical Engineering, University of Massachusetts, Amherst, MA 01003, USA
[b] Department of Chemistry, University of Massachusetts, Amherst, MA 01003, USA

ARTICLE INFO

Article history:
Received 21 July 2009
Revised 21 December 2009
Accepted 1 January 2010
Available online 1 February 2010

Keywords:
Nitrided zeolites
Kinetic stability
Solid base catalyst
Ammonolysis

ABSTRACT

We have modeled the formation kinetics of nitrogen-substituted (nitrided) zeolites HY and silicalite; we have also modeled the stability of nitrided sites to heat and humidity. These kinetic calculations are based on mechanisms computed from DFT-computed pathways reported in our previous work. Reactant ammonia and product water concentrations were fixed at various levels to mimic continuous nitridation reactors. We have found that zeolite nitridation — replacing Si–O–Si and Si–OH–Al linkages with Si–NH–Si and Si–NH_2–Al, respectively — proceeds only at high temperatures (>600 °C for silicalite and >650 °C for HY) due to the presence of large overall barriers. These threshold temperatures are in good agreement with experiments. Nitridation yields were found to be sensitive to water concentration, especially for silicalite where nitridation is more strongly endothermic. As a result, overall nitridation yields in silicalite are predicted to be much lower than those in HY. The stability of nitrided sites was investigated by modeling the kinetics of nitridation in reverse, going back to untreated zeolite plus ammonia. Using 10 h as a benchmark catalyst lifetime, nitrided silicalite and HY half-lives exceeded 10 h for temperatures below 275 and 500 °C, respectively, even at saturation water loadings. As such, our calculations suggest that nitrided silicalite and HY zeolites require high temperatures to form, but once formed, they remain relatively stable, auguring well for their use as shape-selective base catalysts.

1. Introduction

Acidic zeolites have proven to be effective and stable catalysts for a variety of petrochemical and fine-chemical processes [1]. Nitrided zeolites — i.e., those with Si–O–Si and Si–OH–Al groups substituted by Si–NH–Si and Si–NH_2–Al — show promise as shape-selective basic catalysts [2–5]. Such materials may find use in carbon–carbon bond-forming reactions for biofuel production [6], as well as in the fine-chemical, pharmaceutical and food industries [7–10]. However, for nitrided zeolites to be useful catalysts, their stabilities to heat and humidity must be investigated and understood. For example, Ernst et al. found that the presence of water can influence the activity of nitrided zeolites [2]. To shed light on this, we have applied molecular modeling to understand the formation and decomposition kinetics of nitrided zeolites HY and silicalite. In our previous work [11], we used DFT to compute pathways and energetics of nitridation in these zeolites. In the present paper, we apply these mechanisms to develop rate equations describing nitridation rates and yields. We also study the reverse processes to investigate the stability of these nitrided materials to heat and humidity.

Our DFT calculations reveal two-step processes for nitridation of HY and silicalite, but with very different intermediates [11]. The intermediate in silicalite involves a 4-ring $\equiv Si\left\langle \begin{matrix} N \\ O \end{matrix} \right\rangle Si\equiv$ with pentavalent Si, while nitridation in HY involves physisorbed ammonia activated by release from the bidentate ammonium–zeolite ion-pair complex. The overall barriers for nitridation were found to be quite similar in HY and silicalite, around 340–360 kJ/mol, indicating the need for high temperatures during nitridation. However, the reaction energies from gas-phase ammonia to gas-phase water are quite different: 29 kJ/mol for HY and 132 kJ/mol in silicalite, indicating the possibility of higher nitridation yields in HY. Now we turn to making these qualitative statements quantitative by developing kinetic equations that give overall rates and yields.

Our kinetic model is inspired by experimental nitridation, which is typically carried out under high flow rates of dried ammonia at high temperatures (>500 °C) [5,12–14]. We have found in our most recent experimental work that high ammonia flow rates are crucial for generating high-quality nitrided zeolites, with significant nitrogen substitution, good crystallinity and microporosity [14]. The effect of high ammonia flow rates is to keep the concentration of ammonia in zeolite pores high and the concentration of

* Corresponding author. Address: Goesmann 222, University of Massachusetts, Amherst, MA 01003-9336, USA. Fax: +1 413 545 4490.
E-mail addresses: vagarwal@ecs.umass.edu (V. Agarwal), huber@ecs.umass.edu (G.W. Huber), wconner@ecs.umass.edu (W. Curtis Conner Jr.), auerbach@chem.umass.edu (S.M. Auerbach).

0021-9517/$ - see front matter © 2010 Elsevier Inc. All rights reserved.
doi:10.1016/j.jcat.2010.01.001

water low, hence pulling the endothermic equilibrium to nitrided products by LeChatelier's principle.

The combination of high pressure and temperature means that pores are filled with *very* weakly adsorbed ammonia, which we model as a kind of gas-phase or "free" ammonia at fixed concentration in zeolite pores. This "free" intrapore ammonia can evolve to a more bound species of ammonia, ready to engage in nitridation chemistry as described in our previous work [11], involving intermediates, transition states, and eventually products, consisting of the nitrided zeolite plus bound intrapore water. At the temperatures and ammonia flow rates used in nitridation, this bound species of intrapore water will itself evolve to a more "free" form of intrapore water, whose concentration we will model in our kinetic equations as being fixed to various low values. Because the concentrations of these "free" ammonia and water species inside zeolite pores are not known during nitridation, we will investigate below how varying these concentrations influences rates and yields of nitridation. We will also determine how varying the concentration of "free" water impacts stabilities of nitrided zeolites.

By modeling nitridation at fixed concentrations of free ammonia and water, we consider the process at steady state with respect to these weakly adsorbed species. To implement such a model, we require rate constants describing the bimolecular process of binding free ammonia at zeolite Brønsted sites, and free water at zeolite-nitrided sites. Such rate constants can be estimated using gas-phase collision theory, but such a simple approach ignores the nature of intrapore dynamics and diffusion. Molecular dynamics simulations can in principle account for these effects, but such a treatment is beyond the scope of the present work.

Below we find that nitridation yields are sensitive to free water concentration, especially for silicalite where nitridation is more strongly endothermic. Our calculations also suggest that nitrided silicalite and HY zeolites require high temperatures to form, but once formed, they remain relatively stable, auguring well for their use as shape-selective base catalysts.

The remainder of this article is organized as follows: in Section 2 we set up the kinetic equations and give computational details regarding their parameterization and solution; in Section 3 we give results and discussion of both nitridation kinetics and product stability; in Section 4 we offer concluding remarks; and in A we detail the set of kinetic equations solved in our study.

2. Calculation details

Here, we describe the kinetic equations used to model zeolite nitridation and stability. Then, we discuss the computation of temperature-dependent parameters for these kinetic equations.

2.1. Kinetic equations

As discussed above, zeolite nitridation is best carried out by passing dried ammonia at high pressures in a fixed bed of zeolite at high temperatures [14]. The ammonia flow rate is kept high to maintain high concentrations of ammonia and to remove water formed during nitridation. As such, the reactor can be modeled as a semi-batch-reactive separator, analogous to a batch reactive-distillation system [15], acting as a multifunctional reactor where one of the products (water) is selectively removed.

For nitridation of both HY and silicalite, we posit the presence of both "free" and "bound" species of reactant ammonia and product water, as discussed in the Introduction. Also, for both HY and silicalite, nitridation was found to proceed via two-step mechanisms, starting from bound ammonia and leading to bound water [11]. As such, the full process beginning with free ammonia and ending with free water is given by the following *four-step* mechanism:

$$\mathrm{Zeo} + \mathrm{NH_3} \underset{k_{-1}}{\overset{k_1}{\rightleftharpoons}} [\mathrm{Zeo}\ldots\mathrm{NH_3}] \underset{k_{-2}}{\overset{k_2}{\rightleftharpoons}} \mathrm{Int} \underset{k_{-3}}{\overset{k_3}{\rightleftharpoons}} [\mathrm{NH-Zeo}\ldots\mathrm{H_2O}] \underset{k_{-4}}{\overset{k_4}{\rightleftharpoons}} \mathrm{NH-Zeo} + \mathrm{H_2O}. \quad (1)$$

In mechanism (1), "Zeo" represents a possible nitridation site. As discussed in our previous work [11], we have investigated kinetics at the following possible nitridation sites: ≡Si—O—Si≡ at oxygen O(13) in silicalite, and ≡Si—OH—Al≡ at O(1) in HY. The designation "NH-Zeo" in mechanism (1) indicates the corresponding nitrided sites, i.e., ≡Si—NH—Si≡ in silicalite and ≡Si—NH_2—Al≡ in HY. NH_3 signifies *extremely* weakly adsorbed ammonia in silicalite and HY pores, while Zeo…NH_3 indicates ammonia bound to sites in silicalite and HY that we have considered for nitridation in previous work [11]. Likewise, H_2O signifies *extremely* weakly adsorbed water in nitrided silicalite and HY pores, while NH-Zeo…H_2O indicates water bound to nitrided sites in silicalite and HY. Finally, Int labels the nitridation intermediates discussed in our previous work [11]; these are activated molecular ammonia in HY, and a 4-ring ≡Si$<^{\mathrm{N}}_{\mathrm{O}}>$Si≡ with pentavalent Si in silicalite.

The corresponding set of coupled differential equations is given in Appendix A. In these rate equations, we use concentration units of numbers of molecules or sites per unit cell volume. We note that rate equations for free ammonia and water are not present in Appendix A because we hold these concentrations fixed, hence making a steady-state approximation for these species. We also note that the sum of rate equations in Appendix A vanishes, enforcing conservation of mass of the zeolite during nitridation. We solve these rate equations with two different initial conditions to model two distinct experiments. In the first case, we model the nitridation process (denoted "formation") by starting with a certain concentration of Zeo, a fixed high concentration of free ammonia, and various fixed concentrations of free water. In the second case, we model the stability of nitrided catalyst (denoted "stability") by starting with a certain concentration of NH-Zeo, various fixed concentrations of free water, and no free ammonia. This second case investigates the use of nitrided zeolites as catalysts in the presence of various amounts of water.

For *formation* calculations, we report saturated free ammonia concentrations in mmol per gram zeolite, the typical units of experimental adsorption measurements. For all calculations, we report free water concentrations in molecules per unit cell to indicate whether the system is near water saturation or is relatively dilute. For silicalite nitridation at O(13), we assume an initial Zeo concentration of 7.4 sites per unit cell, obtained by dividing the 192 oxygens per MFI unit cell into the 26 crystallographically distinct oxygen locations [16]. The free ammonia concentration in silicalite was fixed at its saturation value of 1.5 mmol/g silicalite (16 molecules per unit cell) [17]. As a point of reference, we note that ammonia becomes saturated at a pressure of 9.8 atm at 25 °C. Free water concentrations for nitridation of silicalite were fixed at values in the range 10^{-6}–10^{-4} molecule per unit cell. As a reference point, these loadings correspond at 800 °C to equilibrium water partial pressures of 4×10^{-7} and 4×10^{-5} atm, respectively. These values were obtained by calculating Henry's law coefficient at 300 °C in the Henry's law regime [18], and extrapolating to 800 °C using the van't Hoff equation. Although drying zeolites so thoroughly is generally difficult, the conditions studied herein of very high temperatures coupled with high flow rates of ammonia make these water concentrations relevant. Nitridation of silicalite was studied at temperatures in the range 700–1000 °C. For both silicalite and HY, calculated nitridation yields are reported as % substitution = $([\mathrm{NH\text{-}Zeo}]_t/[\mathrm{Zeo}]_0) \times 100\%$, for consistency with our recent experimental studies [5,14].

For HY nitridation at O(1), we assume an initial Zeo concentration of 13.5 sites per unit cell, derived as follows. Our recent nitrid-

ation experiments on HY involved a Si:Al ratio of 6.1 [5], corresponding to 27 Brønsted sites (Si–OH–Al) per unit cell. Preferential siting of Brønsted sites in HY at O(1) and O(3) as determined by neutron diffraction [19] and calculations [20] suggests spreading these 27 sites evenly at O(1) and O(3), giving 13.5 sites per unit cell at O(1) before nitridation. The free ammonia concentration in HY was fixed at its saturation value of 2.5 mmol/g HY (35 molecules per unit cell, ammonia partial pressure unknown) [21]. Free water concentrations for nitridation of HY were fixed at values in the range 10^{-5}—10^{-3} molecule per unit cell. The partial pressures of equilibrium water could not be determined due to difficulty in resolving the adsorption isotherm of water in HY in the Henry's law regime. The best estimate of these loadings correspond at 800 °C to equilibrium water partial pressures of 3×10^{-4} and 3×10^{-2} atm, respectively [22]. Nitridation of HY was studied at temperatures in the range 700–1000 °C. As stated above, such low concentrations are relevant at high temperatures and high ammonia flow rates.

Stability calculations for nitrided silicalite and HY were initiated with NH-Zeo concentrations of 5% and 30% substitution, respectively. The stability of nitrided silicalite was modeled with temperatures in the range 250–325 °C, and free water concentrations fixed at values in the range 1–15 molecules per unit cell, the upper limit corresponding to water saturation in silicalite [18]. The stability of nitrided HY was modeled at temperatures in the range 450–550 °C, and with free water concentrations fixed at values in the range 1–200 molecules per unit cell, the upper limit in this case corresponding to water saturation in HY [22]. As a point of reference, we note that water vapor becomes saturated at a pressure of 0.031 atm at 25 °C [18].

The micro-kinetic model leads to a set of simultaneous differential equations. Because of the wide separation in rate constant values (see below), these equations form a "stiff" set of differential equations; this problem arises when some variables change rapidly with time while others change more slowly. For dynamical stability in the solution of the differential equations, the step size must be selected according to the most rapidly changing variable. To increase efficiency, we have used a variable step-size algorithm [23]. In general, the equations were solved to an absolute tolerance of 10^{-6} molecules/cm^3.

2.2. Kinetic parameters

All the rate constants in mechanism (1) are unimolecular except for k_1 and k_{-4}, which are bimolecular because of the independent concentrations of Zeo/NH-Zeo and NH_3/H_2O. In general, we assumed that the rate constants obey the Arrhenius temperature dependence:

$$k = Ae^{-\Delta V/RT}, \tag{2}$$

where A is a pre-exponential factor, ΔV is the activation energy and T is the absolute temperature of the reaction. In our previous work [11], we computed the activation energies for all the unimolecular processes in mechanism (1); these are listed below in Table 1. The unimolecular pre-exponential factors are attempt frequencies that can be computed using, e.g., classical harmonic transition state theory (TST) [24] if the frequencies are known. (*Classical* TST was applied because of the high temperatures studied.) The TST attempt frequency calculation was possible for HY, but not for silicalite, because of computational details discussed in our previous work [11]. In particular, the electronic structure calculations on HY were essentially unconstrained, leading to the correct number of real frequencies at the reactant and transition states. In contrast, the DFT calculations on silicalite had to be constrained to maintain the correct pore structure, leading to incommensurate numbers of real frequencies at reactant and transition states, precluding the application of TST. As such, for the unimolecular processes in silicalite, we made the standard assumption of $A = 10^{13}$ s^{-1} [25]. For the same processes in HY, we applied TST to compute A according to:

$$A_{\mathrm{TST}} = \frac{\omega_1}{2\pi} \prod_{n=2}^{F} \frac{\omega_n^{\mathrm{reac}}}{\omega_n^{\ddagger}}, \tag{3}$$

where $\{\omega\}$ are vibrational frequencies, F is the number of degrees of freedom in the cluster model of HY, "reac" represents the reactant state, and ‡ represents the transition state. The TST-computed pre-exponentials for HY are listed in Table 1; we note that they take values of order 10^{13} s^{-1} as was assumed for silicalite nitridation.

Table 1
Kinetic parameters for various steps of nitridation in HY and silicalite zeolite.

Rate constant[a]	Silicalite		HY	
	A[b]	ΔV (kJ/mol)	Ab	ΔV (kJ/mol)
Unimolecular (s^{-1})				
k_{-1}	10^{13}	41	10^{13}	111
k_2	10^{13}	314	6.2×10^{13}	118
k_{-2}	10^{13}	114	4.0×10^{13}	2
k_3	10^{13}	143	0.49×10^{13}	244
k_{-3}	10^{13}	185	1.0×10^{13}	262
k_4	10^{13}	15	10^{13}	43
Bimolecular formation ($cm^3\ s^{-1}$)				
k_1	$1.0 \times 10^{-11}\sqrt{T}$	0	$1.0 \times 10^{-11}\sqrt{T}$	0
k_{-4}	$9.8 \times 10^{-11}\sqrt{T}$	0	$1.6 \times 10^{-11}\sqrt{T}$	0
Bimolecular stability ($cm^3\ s^{-1}$)				
k_1	$9.8 \times 10^{-11}\sqrt{T}$	0	$1.6 \times 10^{-11}\sqrt{T}$	0
k_{-4}	$1.0 \times 10^{-11}\sqrt{T}$	0	$1.0 \times 10^{-11}\sqrt{T}$	0

[a] $k = Ae^{-\Delta V/RT}$.
[b] The units of A are same as the corresponding kinetic constant.

To complete the parameterization of the kinetic equations, we need to specify the rate constants controlling the zeolite binding of free water and ammonia (k_1 and k_{-4}), and those controlling the release of bound water and ammonia (k_{-1} and k_4). The release processes are analogous to desorption, with rate constants that are also unimolecular. Here we assume pre-exponential factors equal to 10^{13} s^{-1}, and barriers given by the desorption energies computed in our previous work [11], and tabulated below in Table 1.

The binding processes of free water and ammonia are analogous to adsorption, with bimolecular rate constants describing collisions between very weakly adsorbed guest molecules and intrapore zeolite-binding sites. We assumed these processes to be barrierless ($\Delta V = 0$) as is typical for adsorption. In general, a rate constant describing adsorption from the gas-phase to an adsorbed site requires an entropy correction due to translational and rotational degrees of freedom [26–28]. However, in our case, the weakly adsorbed molecules have already lost their translational and rotational degrees of freedom by virtue of being in a densely filled pore.

The bimolecular pre-exponential factors have units of volume per time (cm^3 s^{-1}). Using gas-phase collision theory [29], one can estimate the bimolecular pre-exponential factor according to:

$$A = \langle v\sigma \rangle \approx \langle v \rangle \cdot \langle \sigma \rangle, \tag{4}$$

where $\langle v \rangle$ is the average thermal speed $=\sqrt{8RT/\pi M}$, M is the molecular mass of ammonia (formation) or water (stability), and $\langle \sigma \rangle$ is a binding cross section. If one assumes a "sticking probability" of unity, the binding cross section is simply the geometrical area presented by a zeolite oxygen- or nitrogen-binding site, denoted σ_{site}. We estimated σ_{site} as πd^2, where d is the Si–Si distance in zeolites, of order 3 Å. One thus obtains a gas-phase pre-exponential factor of order 10^{-10} cm^3 s^{-1} at 298 K (25 °C). In what follows we prefer to indicate the temperature dependence explicitly; the gas-

phase pre-exponential factor thus becomes $1.0 \times 10^{-11}\sqrt{T}$ cm^3 s^{-1}, where the units of absolute temperature are already included in cm^3 s^{-1}. This is our reference expression for further discussion.

This base-case treatment ignores the intrapore dynamics of mixtures. For example, we consider the effect of ammonia loading on the back reaction: decomposition of nitrided sites. The back reaction begins with unbound intrapore water binding to a nitrided site in the presence of high ammonia loading. Our present rate expression for this process is independent of ammonia loading, which is our base-case approximation. Although the presence of ammonia may inhibit binding of water to a nitrided site, the same ammonia may inhibit the dissociation of a water-nitrided-site complex. Assuming that these effects cancel is our base-case model. The model properly describes the fact that the rate of bimolecular association of a particular guest is proportional to guest loading and to the fraction of active zeolite surface area. Going beyond this approximation will require molecular dynamics simulations, the subject of a forthcoming publication.

3. Results and discussion

Here, we discuss the results of modeling nitridation kinetics in HY and silicalite. We also present the results of modeling the stabilities of nitrided sites in HY and silicalite.

3.1. Kinetics of formation

We studied the effect of water concentration and temperature on nitridation yields in HY first to compare with experimental data on this system [5,14]. We then used this approach to predict nitridation yields in silicalite.

Fig. 1 shows the effect of water concentration on nitridation yields in HY. We have modeled the effect of water concentration at 800 °C and for 24-h reaction time, typical values for nitridation chemistry [2–5,13,14,30–34]. The yields are plotted as the percentage of O(1) sites present initially, which we have taken as 13.5 sites per unit cell. For a water concentration of 10^{-3} molecules per unit cell, a steady-state yield of 5% is obtained, which grows to ~50% for 5×10^{-4} waters per unit cell. This yield can be pushed to 100% for a concentration less than 5×10^{-6} waters per unit cell (data not shown). This suggests that nitridation yields are sensitive to water concentration, in qualitative agreement with experiments which require ultrapure ammonia [14].

Our recent experiments and modeling of nitridation yields using NMR has shown that, at this temperature for HY (Si:Al = 15.0), all the acid sites are nitrided and even non-acid sites participate in nitridation [14]. Our present modeling results suggest that this will happen for water concentrations as low as 5×10^{-6} molecules per unit cell, indicating that only a trace amount of water was present during the nitridation syntheses [14]. Although such low concentrations of water are very difficult to achieve experimentally in a zeolite under typical conditions, at very high temperatures and high ammonia flow rates these low water concentrations become relevant.

Fig. 2 shows the effect of water concentration on nitridation in silicalite at 800 °C. Yields are plotted as the percentage of O(13) sites present initially (7.4 sites per unit cell). We observe that for 10^{-3} waters per unit cell, only 0.5% sites are substituted. This yield can be pushed to 5% for 10^{-5} waters per unit cell, and to 10% for 5×10^{-6} waters per unit cell. Fig. 2 shows that even a trace amount of water can inhibit nitridation in silicalite. This can be explained by the fact that nitridation in silicalite is more endothermic (132 kJ/mol) than it is in HY (29 kJ/mol), as shown previously [11]. This also accounts for the fact that nitridation yields computed for silicalite are generally lower than those for HY. In principle, silicalite nitridation can be driven to completion by removing all the water; however, this is difficult to achieve in practice, even for a hydrophobic material such as silicalite.

Now, comparing the kinetics of nitridation in silicalite and HY, we find that steady states in silicalite are generally attained much more rapidly than those in HY, for the same water concentration and temperature. This is because, as reported in our previous work [11], the overall barrier for nitridation in silicalite (343 kJ/mol) is lower than that for HY (359 kJ/mol). This difference, 16 kJ/mol, is still significant at 800 °C, which corresponds to thermal energy (RT) of 8.9 kJ/mol.

The effect of temperature on nitridation yields in HY at 10^{-4} waters per unit cell and silicalite at 10^{-5} waters per unit cell are shown in Figs. 3 and 4, respectively. We find that temperatures above 650 °C for HY, and above 600 °C for silicalite, are required to form nitrided zeolites, a result in broad agreement with nitridation experiments on Y [3,5,13,14] and silicalite [31–34]. We find that increasing temperature increases the nitridation yields for the same water concentration during the simulation. Increasing the temperature in HY from 700 °C to 900 °C, increases the nitridation yields from 1% to 85% for the period of 24 h. For silicalite, increasing the temperature from 700 °C to 900 °C increases the nitridation yields from 1% to 20% for a 2-h period.

To summarize, high nitridation yields are predicted by our micro-kinetic model at sufficiently high temperatures and low water

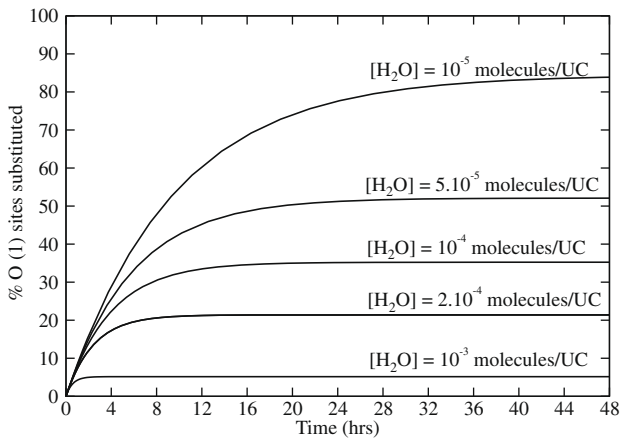

Fig. 1. Effect of water concentration on nitridation yield in HY at T = 800 °C and [NH_3] = 2.5 mmol/g-zeolite.

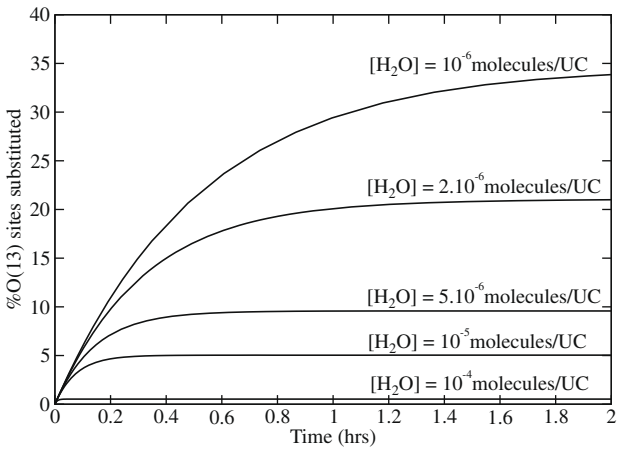

Fig. 2. Effect of water concentration on nitridation yield in silicalite at T = 800 °C and [NH_3] = 1.5 mmol/g-zeolite.

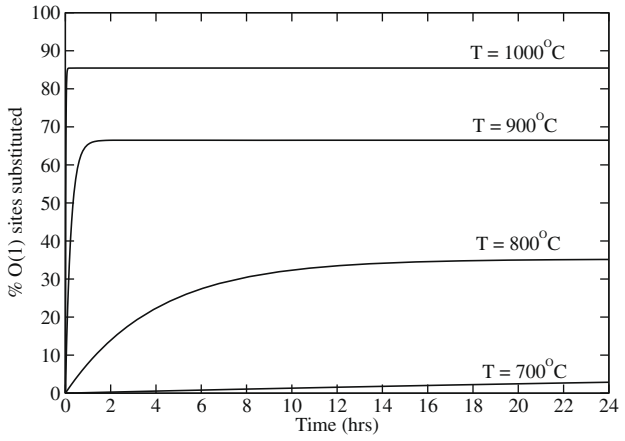

Fig. 3. Effect of temperature on nitridation yield in HY at $[H_2O] = 10^{-4}$ molecules/UC and $[NH_3]$ = 2.5 mmol/g-zeolite.

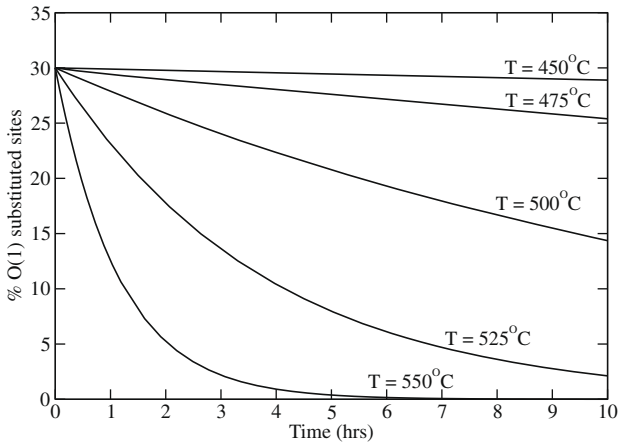

Fig. 5. Effect of temperature on the stability of nitrided sites in HY at $[H_2O]$ = 200 molecules/UC, P_S = 0.0313 atm at 25 °C.

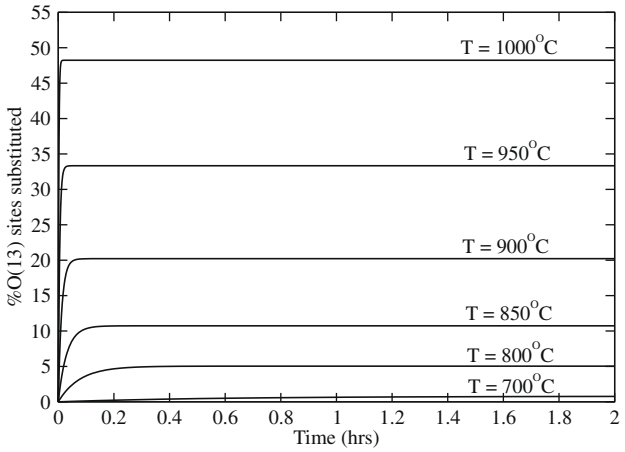

Fig. 4. Effect of temperature on nitridation yield in silicalite at $[H_2O] = 10^{-5}$ molecules/UC and $[NH_3]$ = 1.5 mmol/g-zeolite.

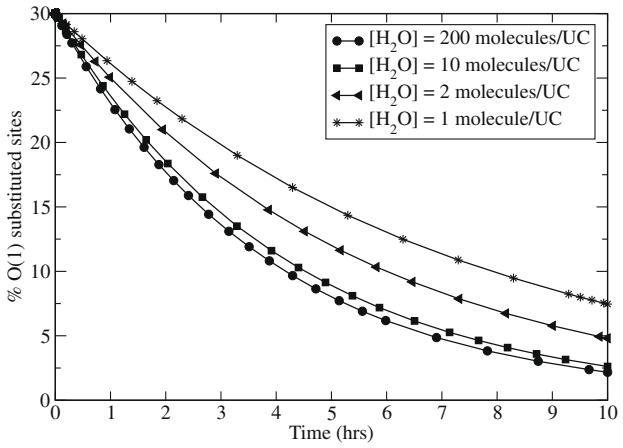

Fig. 6. Effect of water concentration on the stability of nitrided sites in HY at T = 525 °C.

concentrations. Although such high temperatures can cause significant damage to zeolite frameworks, our combined theoretical and experimental studies have shown that nitrided zeolites can still show well-ordered framework structure [5,14]. Nonetheless, finding effective nitridation processes that operate at lower temperatures is desirable because of the need to reduce both framework damage and energy costs.

3.2. Kinetics of stability

We modeled the stability of nitrided zeolites by integrating the kinetic equations with relatively high water loadings, and with essentially no free ammonia, to simulate the use of nitrided zeolites as catalysts in contact with various concentrations of water.

We begin by discussing the effects of temperature and water concentration on the stability of nitrided sites in HY, as shown in Figs. 5 and 6, respectively. The decomposition of nitrided sites is plotted as %NH sites present relative to the initial number of O(1) Brønsted sites in HY (taken as 13.5 sites per unit cell). For the temperature study in Fig. 5, we fixed water concentration at 200 molecules per unit cell, which corresponds to saturation water loadings in HY [22]. Fig. 5 shows that for a period of 10 h, the nitrided sites in HY are quite stable for temperatures less than 450 °C, even for saturation water loadings. The nitrided sites completely decompose in this time period at 550 °C or higher, indicating that stability is very sensitive to temperature above a threshold temperature. Ten hours is predicted to be the half-life of nitrided HY at 500 °C.

Such threshold temperatures can be increased by lowering water concentration, as shown in Fig. 6 for a fixed temperature of 525 °C. We found that nitrided sites decompose from 30% to 2.4% in a period of 10 h for a water concentration of 200 molecules per unit cell. At one water per unit cell, the stability improves falling only to 7.5% after 10 h. Such stabilization also arises at 515 °C and saturation water loadings.

In Figs. 7 and 8 we show the effects of temperature and water concentration, respectively, on the decomposition of nitrided sites plotted as %NH sites present relative to the initial number of O(13) sites in silicalite (taken as 7.4 sites per unit cell). For the temperature study in Fig. 7, we fixed water concentration at 15 molecules per unit cell, which corresponds to saturation water loadings in silicalite [18].

We found that for a period of 10 h, the nitrided sites in silicalite are quite stable for temperatures of less than 250 °C, even for saturation water loadings. The nitrided sites completely decompose in this time period for temperatures of 300 °C or higher, again indicating sensitivity to heat. For comparison, we note that higher temperatures (>525 °C) are required for decomposing nitrided sites in HY as compared to those in silicalite (>300 °C), within our standard 10-h time frame. One can explain this on the basis that the reaction

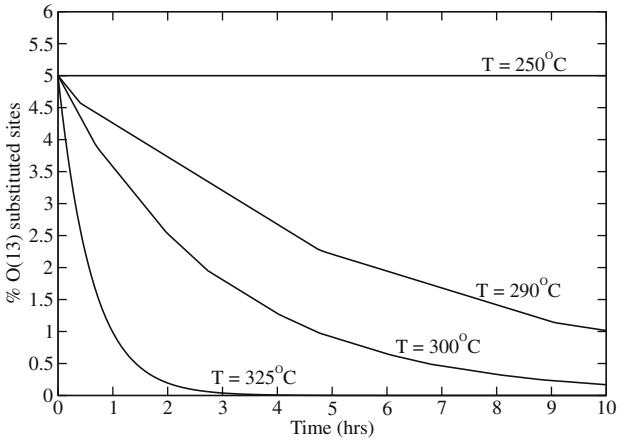

Fig. 7. Effect of temperature on the stability of nitrided sites in silicalite at $[H_2O]$ = 15 molecules/UC, P_S = 0.0313 atm at 25 °C.

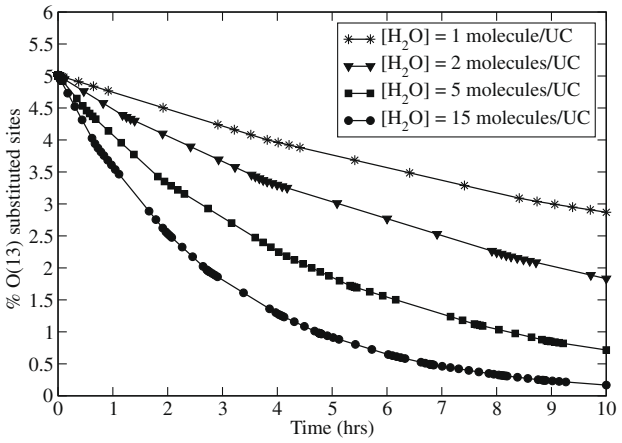

Fig. 8. Effect of water concentration on the stability of nitrided sites in silicalite at T = 300 °C.

barrier for decomposition of nitrided sites is lower for silicalite (185 kJ/mol) as compared to HY (262 kJ/mol), as reported in our previous work [11].

As with HY, we find again with silicalite that decreasing water concentrations pushes stability temperatures to higher values, as shown in Fig. 8 at 300 °C. For example, nitrided sites that were decomposed almost completely within 10 h at water saturation are decomposed only halfway for a water concentration of 2 molecules per unit cell.

To summarize, both heat and humidity are detrimental to nitrided sites in HY and silicalite. We find that site stability is very sensitive to temperature above threshold temperatures (>500 °C for HY and >275 °C for silicalite).

4. Concluding remarks

We have modeled the formation kinetics of nitrogen-substituted (nitrided) zeolites HY and silicalite; we have also modeled the stability of nitrided sites to heat and humidity. We have performed these kinetics calculations on the basis of mechanisms from DFT-computed pathways reported in our previous work. In order to mimic continuous flow reactors used for nitridation, reactant ammonia and product water concentrations were fixed at various levels. We have found that zeolite nitridation proceeds only at high temperatures (>600 °C for silicalite and >650 °C for HY) due to the presence of large overall barriers computed in previous work. These threshold temperatures are in broad agreement with experiments.

Nitridation yields were found to be sensitive to water concentration, especially for silicalite where nitridation is more strongly endothermic. As a result, overall nitridation yields in silicalite are predicted to be lower than those in HY. The stability of nitrided sites was investigated by modeling the kinetics of nitridation in reverse, going back to untreated zeolite plus ammonia. Using 10 h as a benchmark catalyst lifetime, nitrided silicalite and HY half-lives exceed 10 h for temperatures below 275 and 500 °C, respectively, even at saturation water loadings. As such, our calculations suggest that nitrided silicalite and HY zeolites require high temperatures to form, but once formed, they remain relatively stable, suggesting that these materials may be useful as shape-selective base catalysts.

Future work includes measurements of base strength in nitrided zeolites and measurements of site stability to test the predictions made herein. Ultimately, work on determining mechanisms of reactions catalyzed by nitrided zeolites will be crucial for rational design of these shape-selective base catalysts.

Acknowledgments

We thank K. Hammond, Dr. G. Tompsett and Dr. J. T. Fermann at UMass Amherst; Dr. T. Vreven at UMass Worcester; and Dr. D. Fox at Gaussian, Inc. for their expertise. We also thank Prof. C. Grey and F. Dogan at Stony Brook University for stimulating discussions and collaborations on nitrided zeolites. We are grateful for generous funding from the National Science Foundation (CBET-0553577) and the Department of Energy (DEFG027ER15918).

Appendix A. Kinetic equations

The complete micro-kinetic model of mechanism 1 would involve rate equations for seven species: Zeo, Zeo...NH_3, Int, NH-Zeo...H_2O, NH-Zeo, NH_3, and H_2O. However, the experiments we are modeling effectively keep $[NH_3]$ and $[H_2O]$ at constant levels because of high ammonia flow rates involved. This kind of steady state reactor condition is denoted as a semi-batch-reactive separator, because the zeolite remains in the reactor (semi-batch), while the H_2O is removed under NH_3 flow (separator). The equations for this reactor are as follows:

$$\frac{d[\text{Zeo}]}{dt} = -k_1[\text{Zeo}][\text{NH}_3] + k_{-1}[\text{Zeo}\ldots\text{NH}_3] \tag{A.1}$$

$$\frac{d[\text{Zeo}\ldots\text{NH}_3]}{dt} = k_1[\text{Zeo}][\text{NH}_3] - (k_{-1}+k_2)[\text{Zeo}\ldots\text{NH}_3] + k_{-2}[\text{Int}] \tag{A.2}$$

$$\frac{d[\text{Int}]}{dt} = k_2[\text{Zeo}\ldots\text{NH}_3] - (k_{-2}+k_3)[\text{Int}] + k_{-3}[\text{NH}-\text{Zeo}\ldots\text{H}_2\text{O}] \tag{A.3}$$

$$\frac{d[\text{NH}-\text{Zeo}\ldots\text{H}_2\text{O}]}{dt} = k_3[\text{Int}] - (k_{-3}+k_4)[\text{NH}-\text{Zeo}\ldots\text{H}_2\text{O}] + k_{-4}[\text{NH}-\text{Zeo}][\text{H}_2\text{O}] \tag{A.4}$$

$$\frac{d[\text{NH}-\text{Zeo}]}{dt} = k_4[\text{NH}-\text{Zeo}\ldots\text{H}_2\text{O}] - k_{-4}[\text{NH}-\text{Zeo}][\text{H}_2\text{O}] \tag{A.5}$$

Concentration units are numbers of molecules (ammonia or water) or sites (Zeo or NH-Zeo) per unit cell volume. The sum of the rates above vanishes, enforcing conservation of zeolite mass. We solve these rate equations forward to model nitridation (denoted "formation") and backwards to model catalyst "stability". This micro-kinetic model leads to a set of "stiff" differential equations, because some concentrations vary much more rapidly than

others. To increase efficiency, we have used a variable step-size algorithm [23], solving the equations to an absolute tolerance of 10^{-6} molecules/cm^3.

References

[1] S.M. Auerbach, K.A. Carrado, P.K. Dutta, Handbook of Zeolite Science and Technology, Marcel Dekker, Inc., New York, 2003.

[2] S. Ernst, M. Hartmann, T. Hecht, P.C. Jaen, S. Sauerbeck, The influence of water on the activity of nitridated zeolites in base-catalyzed reactions, in: R. Aiello, G. Giordano, F. Testa (Eds.), Impact of Zeolites and Other Porous Materials on the New Technologies at the Beginning of the New Millennium, Parts A and B, Studies in Surface Science and Catalysis, vol. 142, 2002, pp. 549–556. 2nd International Conference of the Federation-of-European-Zeolite-Associations, Taormina, Italy, September 01–05, 2002.

[3] M. Srasra, G. Poncelet, P. Grange, S. Delsarte, Nitrided ultrastable zeolite Y: identification and quantification of incorporated nitrogen species and their influence on the basic catalytic activity, in: J. Cejka, N. Zilkova, P. Nachtigall (Eds.), Molecular Sieves: From Basic Research to Industrial Applications, Parts A and B, Studies in Surface Science and Catalysis, vol. 158, 2005, pp. 1811–1818. 3rd Conference of the Czech Republic, August 23–29, 2005.

[4] K. Narasimharao, M. Hartmann, H.H. Thiel, S. Ernst, Novel solid basic catalysts by nitridation of zeolite beta at low temperature, Microporous and Mesoporous Materials 90 (1–3) (2006) 377–383.

[5] K.D. Hammond, F. Dogan, G.A. Tompsett, V. Agarwal, J.W. Curtis Conner, C.P. Grey, S.M. Auerbach, Spectroscopic signatures of nitrogen substituted zeolites, Journal of American Chemical Society 130 (45) (2008) 14912–14913.

[6] G.W. Huber, S. Iborra, A. Corma, Synthesis of transportation fuels from biomass: chemistry, catalysts, and engineering, Chemical Reviews 106 (9) (2006) 4044–4098.

[7] H. Hattori, Heterogeneous basic catalysis, Chemical Reviews 95 (3) (1995) 537–558.

[8] Y. Ono, T. Baba, Selective reactions over solid base catalysts, Catalysis Today 38 (3) (1997) 321–337. International Symposium on Acid–Base Catalysis III, Rolduc, Netherlands, April 20–24, 1997.

[9] J. Weitkamp, M. Hunger, U. Rymsa, Base catalysis on microporous and mesoporous materials: recent progress and perspectives, Microporous and Mesoporous Materials 48 (1–3) (2001) 255–270 (special issue). International Symposium on Zeolite and Microporous Crystals 2000 (Zmpc 2000), Sendai, Japan, August 06–09, 2000.

[10] Y. Ono, Solid base catalysts for the synthesis of fine chemicals, Journal of Catalysis 216 (1–2) (2003) 406–415.

[11] V. Agarwal, G.W. Huber, J.W. Curtis Conner, S.M. Auerbach, DFT study of nitrided zeolites: mechanism of nitrogen substitution in HY and silicalite, Journal of Catalysis 269 (2010) 53–63.

[12] G.T. Kerr, G.F. Shipman, Reaction of hydrogen Zeolite Y with ammonia at elevated temperatures, Journal of Physical Chemistry 72 (8) (1968) 3071–&.

[13] S. Ernst, M. Hartmann, S. Sauerbeck, T. Bongers, A novel family of solid basic catalysts obtained by nitridation of crystalline microporous aluminosilicates and aluminophosphates, Applied Catalysis A: General 200 (1–2) (2000) 117–123.

[14] F. Dogan, K.D. Hammond, G.A. Tompsett, H. Huo, J.W. Curtis Conner, S.M. Auerbach, C.P. Grey, earching for microporous, strongly basic catalysts: experimental and calculated ^{29}Si NMR spectra of heavily nitrogen-doped Y zeolites, Journal of the American Chemical Society 131 (31) (2009) 11062–11079.

[15] V. Agarwal, S. Thotla, S.M. Mahajani, Attainable regions of reactive distillation — part I. Single reactant non-azeotropic systems, Chemical Engineering Science 63 (11) (2008) 2946–2965.

[16] H. van Koningsveld, High-temperature (350-K) orthorhombic framework structure af zeolite H-ZSM-5, Acta Crystallographica Section B: Structural Science 46 (Part 6) (1990) 731–735.

[17] S. Bordiga, A. Damin, F. Bonino, A. Zecchina, G. Spano, F. Rivetti, V. Bolis, C. Prestipino, C. Lamberti, Effect of interaction with H_2O and NH_3 on the vibrational, electronic, and energetic peculiarities of Ti(IV) centers TS-1 catalysts: a spectroscopic and computational study, Journal of Physical Chemistry B 106 (38) (2002) 9892–9905.

[18] E.M. Flanigen, J.M. Bennett, R.W. Grose, J.P. Cohen, R.L. Patton, R.M. Kirchner, J.V. Smith, Silicalite, a new hydrophobic crystalline silica molecular-sieve, Nature 271 (5645) (1978) 512–516.

[19] M. Czjzek, H. Jobic, A.N. Fitch, T. Vogt, Direct determination of proton positions in D–Y and H–Y zeolite samples by neutron powder diffraction, Journal of Physical Chemistry 96 (1992) 1535–1540.

[20] J.T. Fermann, T. Moniz, O. Kiowski, T.J. McIntire, S.M. Auerbach, T. Vreven, M.J. Frisch, Modeling proton transfer in zeolites: convergence behavior of embedded and constrained cluster calculations, Journal of Chemical Theory and Computation 1 (6) (2005) 1232–1239.

[21] I.V. Mishin, T.R. Brueva, G.I. Kapustin, Heats of adsorption of ammonia and correlation of activity and acidity in heterogeneous catalysis, Adsorption — Journal of the International Adsorption Society 11 (3–4) (2005) 415–424.

[22] M.M. Dubinin, A.A. Isirikyan, N.I. Regent, K.K. Baier, I.M. Belenkaya, Heat of adsorption of water vapors and benzene on high-silicon zeolite of the faujasite type, Bulletin of the Academy of Sciences of the USSR Division of Chemical Science 36 (3, Part 1) (1987) 437–444.

[23] S.K. Gupta, Numerical Methods for Engineers, Wiley Eastern, New Delhi, 1995.

[24] G.H. Vineyard, Frequency factors and isotope effects in solid state rate processes, Journal of Physics and Chemistry of Solids 3 (1–2) (1957) 121–127.

[25] I. Chorkendorff, J.W. Niemantsverdriet, Concepts of Modern Catalysis and Kinetics, Wiley-VCH Verkag GmbH & Co., Weinheim, 2003.

[26] C. Kemball, Entropy of adsorption, Advances in Catalysis 2 (1950) 233–250.

[27] J.A. Cusumano, M.J.D. Low, Interactions between surface hydroxyl groups and adsorbed molecules. I. The thermodynamics of benzene adsorption, Journal of Physical Chemistry 74 (4) (1970) 792–797.

[28] R.P. Marathe, Investigating entropy changes during gas adsorption in ETS-4, Journal of Colloid and Interface Science 290 (1) (2005) 69–75.

[29] A. Fernandez-Ramos, J.A. Miller, S.J. Klippenstein, D.G. Truhlar, Modeling the kinetics of bimolecular reactions, Chemical Reviews 106 (11) (2006) 4518–4584.

[30] P. Fink, J. Datka, Infrared spectroscopic studies of amination of ZSM-5 zeolites, Journal of the Chemical Society — Faraday Transactions I 85 (Part 10) (1989) 3079–3086.

[31] A.J. Han, Y. Zeng, J. Guo, Y.F. Huang, H.Y. He, Y.C. Long, Interaction of methylamine with highly siliceous MFI, FAU and FER-type zeolites, Chinese Journal of Chemistry 23 (4) (2005) 413–417.

[32] A.J. Han, H.Y. He, J. Guo, H. Yu, Y.F. Huang, Y.C. Long, Studies on structure and acid–base properties of high silica MFI-type zeolite modified with methylamine, Microporous and Mesoporous Materials 79 (1–3) (2005) 177–184.

[33] A.J. Han, J. Guo, H. Yu, Y. Zeng, Y.F. Huang, H.Y. He, Y.C. Long, The leading role of association in framework modification of highly siliceous zeolites with adsorbed methylamine, Chemphyschem 7 (3) (2006) 607–613.

[34] J. Guo, A.-J. Han, H. Yu, J.-P. Dong, H. He, Y.-C. Long, Base property of high silica MFI zeolites modified with various alkyl amines, Microporous and Mesoporous Materials 94 (1–3) (2006) 166–172.